

## Supplementary Materials

Dual-Template Ordered Mesoporous Carbon/Fe<sub>2</sub>O<sub>3</sub> Nanowires as Lithium-ion Battery Anodes

*Junkai Hu, Chuan-Fu Sun, Eleanor Gillette, Zhe Gui, YuHuang Wang\*, and Sang Bok Lee\**

### 1. Calculations

The absolute ( $\Delta V_{meso}$ ) and relative ( $\Delta V_{meso} \%$ ) mesoporous volume difference between OMC/Fe<sub>2</sub>O<sub>3</sub> composites and their corresponding OMCs were calculated through the following equations:

$$\Delta V_{meso} = V_{meso-C} - V_{meso-CFe} / (1 - Fe_2O_3 \text{ wt}\%)$$

(S1)

$$\Delta V_{meso} \% = \frac{\Delta V_{meso}}{V_{meso-C}} \times 100$$

(S2)

Here,  $V_{meso-CFe}$  and  $V_{meso-C}$  are mesopore volume of OMC/Fe<sub>2</sub>O<sub>3</sub> composites and mesopore volume of pure OMCs;  $Fe_2O_3 \text{ wt}\%$  is the mass percentage of Fe<sub>2</sub>O<sub>3</sub> in the OMC/Fe<sub>2</sub>O<sub>3</sub> composites;  $V_{meso-CFe} / (1 - Fe_2O_3 \text{ wt}\%)$  is the mesopore volume of OMC/Fe<sub>2</sub>O<sub>3</sub> composites normalized by the initial carbon mass.

## 2. Figures and Tables

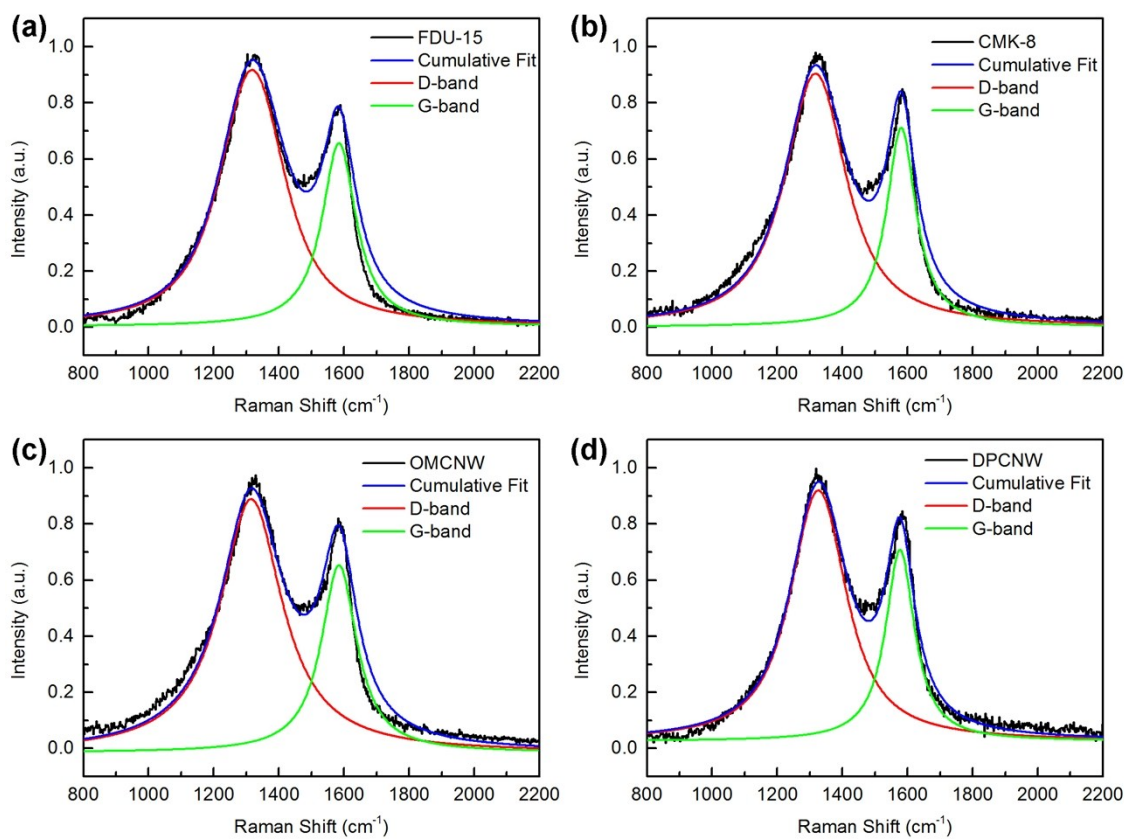


**Figure S1.** De-convoluted Raman D and G bands of (a) FDU-15, (b) CMK-8, (c) OMCNW, and (d) DPCNW.

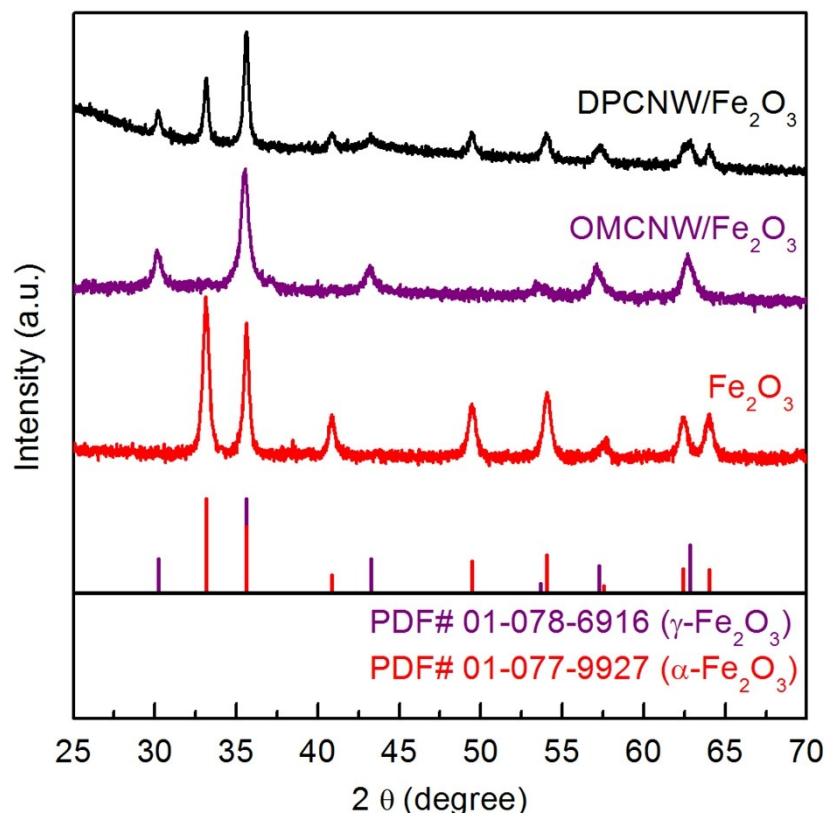


**Figure S2.** XRD spectra of OMCNW/Fe<sub>2</sub>O<sub>3</sub>, DPCNW/Fe<sub>2</sub>O<sub>3</sub>, and Fe<sub>2</sub>O<sub>3</sub>. The standard peaks of  $\gamma$ -Fe<sub>2</sub>O<sub>3</sub> and  $\alpha$ -Fe<sub>2</sub>O<sub>3</sub> are given in the bottom panel. The Fe<sub>2</sub>O<sub>3</sub> sample is synthesized by directly annealing Fe(NO<sub>3</sub>)<sub>3</sub> • 9H<sub>2</sub>O without adding any carbon materials. The anneal process is the same as that for OMC/Fe<sub>2</sub>O<sub>3</sub>.

The carbon-free Fe<sub>2</sub>O<sub>3</sub> shows a pure alpha phase, indicating the decomposed product of Fe(NO<sub>3</sub>)<sub>3</sub> • 9H<sub>2</sub>O is  $\alpha$ -Fe<sub>2</sub>O<sub>3</sub>. However, it is known in the literature that the alpha phase transforms to gamma phase when carbon is introduced into the system, which is very likely due to the interaction of carbon with Fe(NO<sub>3</sub>)<sub>3</sub> during the decomposition process.<sup>1-4</sup> The Fe<sub>2</sub>O<sub>3</sub> in OMCNW/Fe<sub>2</sub>O<sub>3</sub> and other OMC/Fe<sub>2</sub>O<sub>3</sub> composites in this work are  $\gamma$ -Fe<sub>2</sub>O<sub>3</sub>. In the case of DPCNW/Fe<sub>2</sub>O<sub>3</sub>, the outer surface of Fe<sub>2</sub>O<sub>3</sub> particles are in contact with carbon and formed  $\gamma$ -Fe<sub>2</sub>O<sub>3</sub> on the outer surface, whereas the inner parts of Fe<sub>2</sub>O<sub>3</sub> particles do not directly interact with carbon due to the large particle size. Therefore, the Fe<sub>2</sub>O<sub>3</sub> particles inside of DPCNW show mixed phases of  $\alpha$ -Fe<sub>2</sub>O<sub>3</sub> and  $\gamma$ -Fe<sub>2</sub>O<sub>3</sub>.

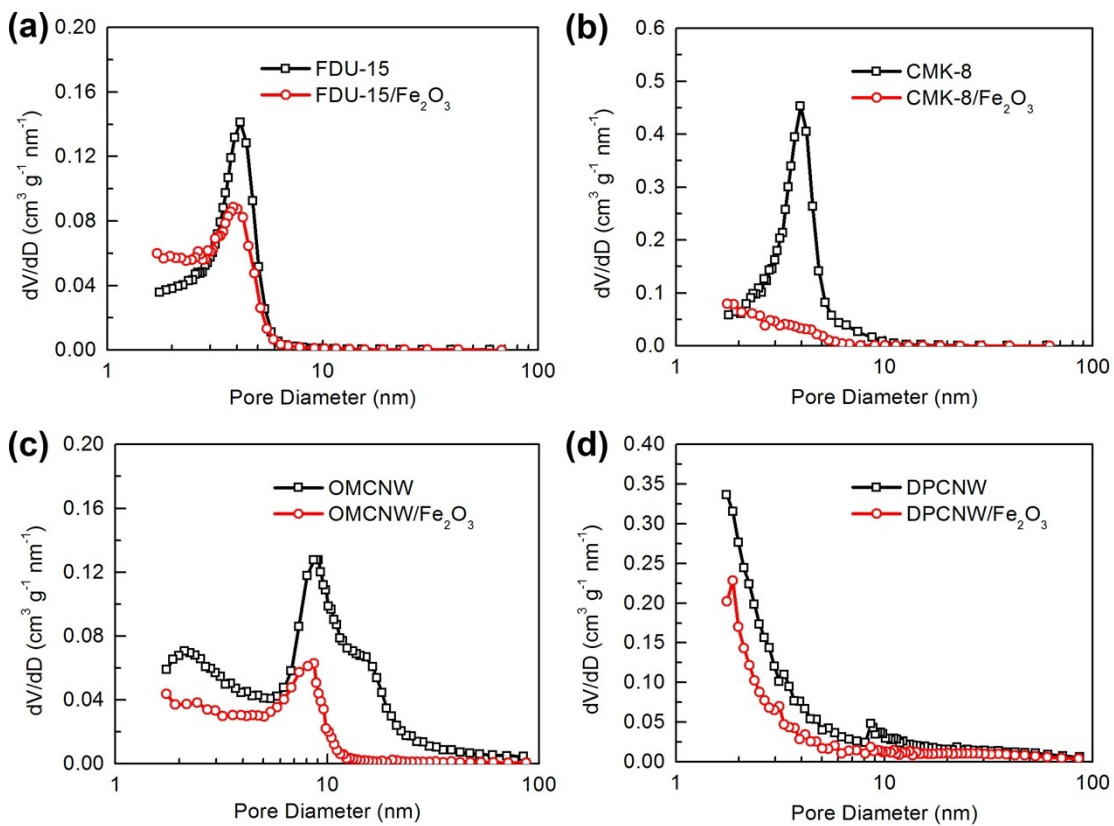


**Figure S3.** Pore size distributions of porous carbons and carbon/Fe<sub>2</sub>O<sub>3</sub> composites.

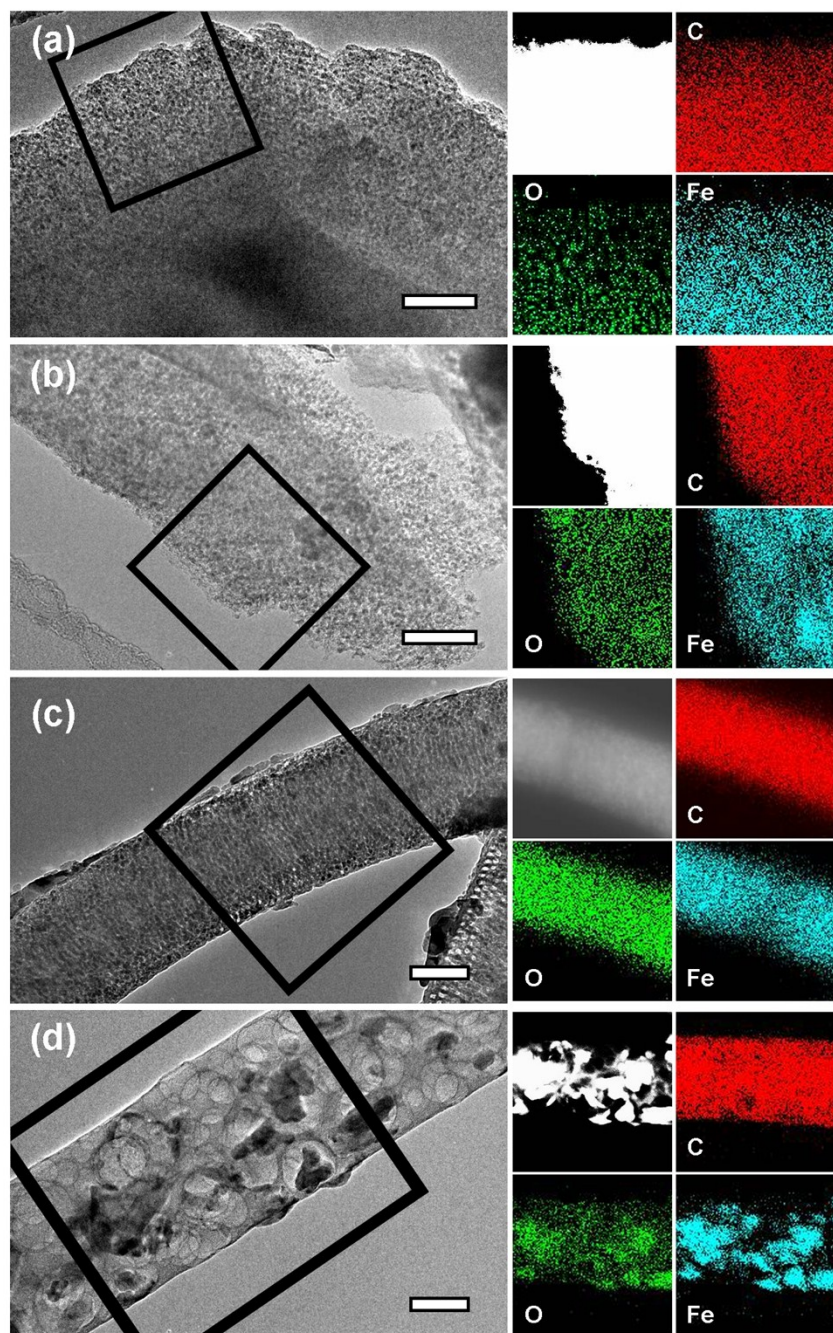


**Figure S4.** TEM images (left) and EDX mappings (right) of (a) FDU-15/Fe<sub>2</sub>O<sub>3</sub>, (b) CMK-8/Fe<sub>2</sub>O<sub>3</sub>, (c) OMCNW/Fe<sub>2</sub>O<sub>3</sub>, and (d) DPCNW/Fe<sub>2</sub>O<sub>3</sub>. All scale bars in the TEM images are 100 nm. The black squares in TEM images are the spots where EDX were taken. The carbon, oxygen, and iron in EDX mappings were represented by red, green, and blue colors, respectively.



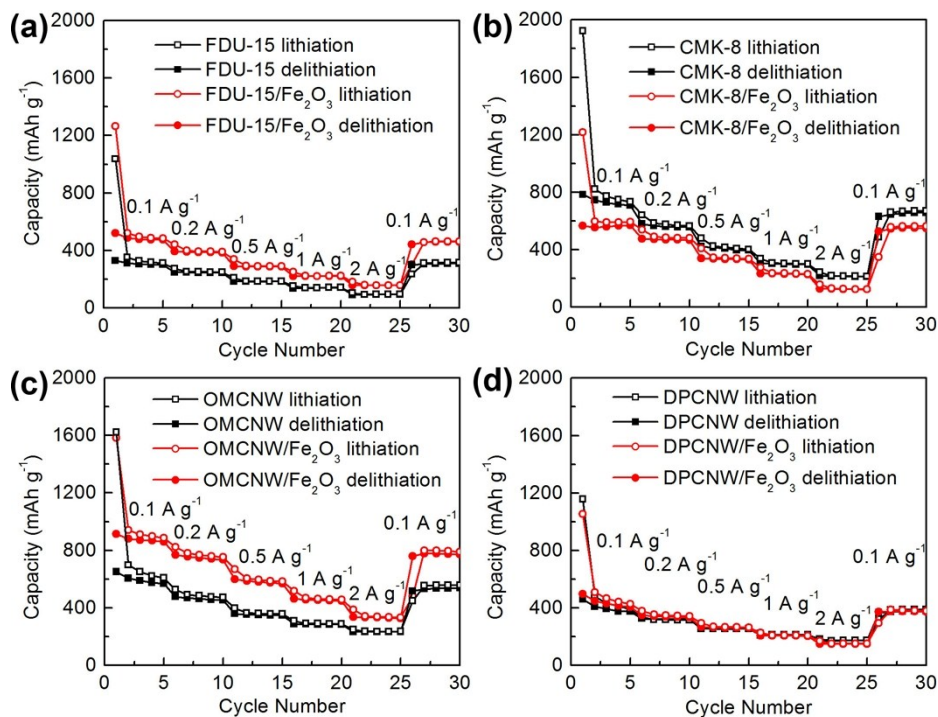


**Figure S5.** Comparison of rate performances of (a) FDU-15 and FDU-15/Fe<sub>2</sub>O<sub>3</sub>, (b) CMK-8 and CMK-8/Fe<sub>2</sub>O<sub>3</sub>, (c) OMCNW and OMCNW/Fe<sub>2</sub>O<sub>3</sub>, and (d) DPCNW and DPCNW/Fe<sub>2</sub>O<sub>3</sub>. Solid: lithiation; open: delithiation.

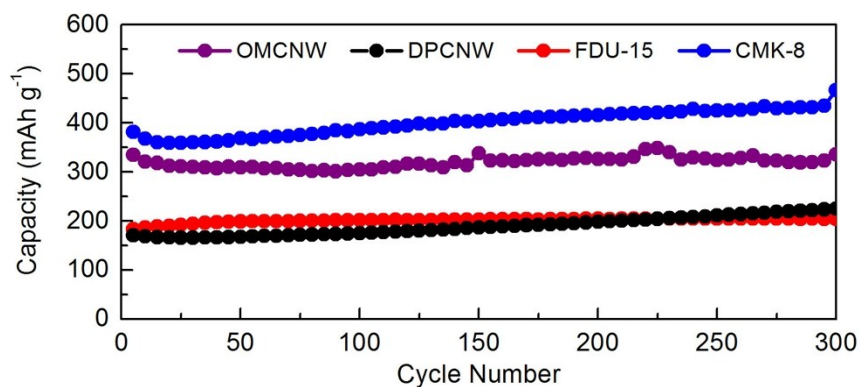


**Figure S6.** Electrochemical cycling performances of FDU-15, CMK-8, DPCNW, and OMCNW. The first 3 cycles are at 0.1 A g<sup>-1</sup> for activation of electrodes (For clarity, data are not shown).

Table S1. EIS parameters for different carbon/Fe<sub>2</sub>O<sub>3</sub> composites

Sample ID	R <sub>s</sub> (Ω)	R <sub>SEI+ct</sub> (Ω)	Z (Ω)
OMCNW/Fe <sub>2</sub> O <sub>3</sub>	3	64	18
FDU-15/Fe <sub>2</sub> O <sub>3</sub>	4	69	47
DPCNW/Fe <sub>2</sub> O <sub>3</sub>	3	139	31
CMK-8/Fe <sub>2</sub> O <sub>3</sub>	3	168	88

Table S2. Estimated volume changes during lithiation process in carbon/Fe<sub>2</sub>O<sub>3</sub> composites.

Sample ID	V <sub>Fe<sub>2</sub>O<sub>3</sub></sub> (cm <sup>3</sup> g <sup>-1</sup> )	ΔV <sub>Fe<sub>2</sub>O<sub>3</sub></sub> (cm <sup>3</sup> g <sup>-1</sup> )	V <sub>C</sub> (cm <sup>3</sup> g <sup>-1</sup> )	ΔV <sub>C</sub> (cm <sup>3</sup> g <sup>-1</sup> )	ΔV <sub>t</sub> (cm <sup>3</sup> g <sup>-1</sup> )	V <sub>t</sub> (cm <sup>3</sup> g <sup>-1</sup> )	ΔV <sub>t</sub> /V <sub>t</sub>
OMCNW/Fe <sub>2</sub> O <sub>3</sub>	0.0858	0.172	0.24	0.024	0.196	0.444	44 %
FDU-15/Fe <sub>2</sub> O <sub>3</sub>	0.0288	0.058	0.38	0.037	0.095	0.264	36 %
DPCNW/Fe <sub>2</sub> O <sub>3</sub>	0.0361	0.072	0.36	0.036	0.108	0.157	69 %
CMK-8/Fe <sub>2</sub> O <sub>3</sub>	0.0683	0.137	0.28	0.028	0.165	0.175	94 %

V<sub>Fe<sub>2</sub>O<sub>3</sub></sub>: Fe<sub>2</sub>O<sub>3</sub> volume based on Fe<sub>2</sub>O<sub>3</sub> density of 5.242 g cm<sup>-3</sup>;

V<sub>C</sub>: carbon volume based on graphite density of 2.267 g cm<sup>-3</sup>;

ΔV<sub>Fe<sub>2</sub>O<sub>3</sub></sub>: Fe<sub>2</sub>O<sub>3</sub> volume expansion estimated from 200 % Fe<sub>2</sub>O<sub>3</sub> volume increase;<sup>5</sup>

ΔV<sub>C</sub>: carbon volume expansion estimated from 10 % graphite volume increase;<sup>6</sup>

ΔV<sub>t</sub>: total volume expansion from ΔV<sub>Fe<sub>2</sub>O<sub>3</sub></sub> and ΔV<sub>C</sub>;

V<sub>t</sub>: total volume from N<sub>2</sub> sorption-desorption;

ΔV<sub>t</sub>/V<sub>t</sub>: ration between changed volume and total volume.

## References

1. I. Kim, G. Nunnery, K. Jacob, J. Schwartz, X. Liu and R. Tannenbaum, *Journal of Physical Chemistry C*, 2010, **114**, 6944-6951.
2. T. Tsoufis, Z. Syrgiannis, N. Akhtar, M. Prato, F. Katsaros, Z. Sideratou, A. Kouloumpis, D. Gournis and P. Rudolf, *Nanoscale*, 2015, **7**, 8995-9003.
3. I. Kim, A. Magasinski, K. Jacob, G. Yushin and R. Tannenbaum, *Carbon*, 2013, **52**, 56-64.
4. N. Liu, J. Shen and D. Liu, *Electrochimica Acta*, 2013, **97**, 271-277.
5. F. Han, D. Li, W.-C. Li, C. Lei, Q. Sun and A.-H. Lu, *Advanced Functional Materials*, 2013, **23**, 1692-1700.
6. Y. Qi, H. B. Guo, L. G. Hector and A. Timmons, *Journal of the Electrochemical Society*, 2010, **157**, A558-A566.